Separation Science and Technology
Publication details, including instructions for authors and subscription information:
http://www.informaworld.com/smpp/title~content=t713708471

Groundwater Cleanup by In-Situ Sparging. VII. Volatile Organic Compounds Concentration Rebound Caused by Diffusion after Shutdown

César Gómez-Lahoz[a]; José M. Rodríguez-Maroto[a]; David J. Wilson[a]
[a] DEPARTAMENTO DE INGENIERÍA QUÍMICA FACULTAD DE CIENCIAS CAMPUS UNIVERSITARIO DE TEATINOS, UNIVERSIDAD DE MÁLAGA, MÁLAGA, SPAIN

To cite this Article Gómez-Lahoz, César , Rodríguez-Maroto, José M. and Wilson, David J.(1994) 'Groundwater Cleanup by In-Situ Sparging. VII. Volatile Organic Compounds Concentration Rebound Caused by Diffusion after Shutdown', Separation Science and Technology, 29: 12, 1509 — 1528
To link to this Article: DOI: 10.1080/01496399408007371
URL: http://dx.doi.org/10.1080/01496399408007371

SEPARATION SCIENCE AND TECHNOLOGY, **29**(12), pp. 1509–1528, 1994

Groundwater Cleanup by In-Situ Sparging. VII. Volatile Organic Compounds Concentration Rebound Caused by Diffusion after Shutdown

CÉSAR GÓMEZ-LAHOZ, JOSÉ M. RODRÍGUEZ-MAROTO, and DAVID J. WILSON*
DEPARTAMENTO DE INGENIERÍA QUÍMICA
FACULTAD DE CIENCIAS
CAMPUS UNIVERSITARIO DE TEATINOS
UNIVERSIDAD DE MÁLAGA
29071 MÁLAGA, SPAIN

ABSTRACT

The sparging of aquifers contaminated with volatile organic compounds (VOCs) is examined by means of a mathematical model which includes the kinetics of solution of nonaqueous phase liquid (NAPL) droplets and of diffusion of VOCs from porous layers of low permeability. The well configuration is that of a single vertical well screened only near the bottom. The dependence of cleanup rates on model parameters (well depth, air flow rate, NAPL droplet diameter, thickness of low-permeability structures, etc.) is reported. The rebound of VOC concentration in the mobile aqueous phase after the sparging well is shut down is examined. Model runs require only a few minutes of computer time on currently available microcomputers.

INTRODUCTION

Sparging is one of the more promising of the innovative technologies being used for the remediation of hazardous waste sites which are contaminated with volatile organic compounds (VOCs). In contrast to soil vapor extraction (SVE), sparging is designed for the removal of VOCs from the

* Permanent address: Department of Chemistry, Box 1822 Sta. B, Vanderbilt University, Nashville, Tennessee 37235, USA.

zone of saturation. Brown has provided an excellent introduction to the technique (1), and a recent EPA report includes articles on the technique (2).

In the present paper we extend the modeling of solution/diffusion process kinetics in in-situ sparging to single vertical wells screened for a short distance at the bottom of the well. We build here on a similar model for sparging of VOCs from aquifers by means of a buried horizontal slotted pipe (3). The reader is referred to Reference 3 for an introduction to the sparging process and an extensive review of the sparging literature. The notation employed there will also be used here; exceptions will be indicated as they arise.

In the following sections we first present a somewhat abbreviated version of the analysis leading to the differential equations constituting the model [to avoid excessive repetition of material covered previously (3)]. This is followed by a discussion of the results of calculations done using the model; we look first at a comparison of sparging by means of a single vertical well with sparging by means of a horizontal slotted pipe. The dependence of cleanup rates on a few of the model parameters is then explored. The section closes with an examination of the rebound of VOC concentration in the mobile aqueous phase when the sparging well is shut down after various periods of operation. A short section on conclusions then completes the paper.

THEORETICAL

The Physical System

A schematic diagram of a sparging setup having the configuration of a single vertical well is shown in Fig. 1. We assume that the aquifer medium is homogeneous and isotropic, so that the system has axial symmetry and we may work in cylindrical coordinates (r, z).

We assume that there are low-permeability porous lenses (clay, till, silt) distributed throughout the aquifer which may contain VOC either dissolved in the immobile water in the porosity of the lenses or actually present as nonaqueous phase liquid (NAPL) droplets. As in our previous model (3), mass transport kinetics limitations can occur via the rate of solution of the droplets and/or the rate of diffusion of dissolved VOC through the immobile water to the mobile water flowing through the more permeable matrix in which the lenses are located.

The injected air is assumed to be at local equilibrium with the mobile water with respect to VOC mass transport, and this equilibrium is assumed to be governed by Henry's law.

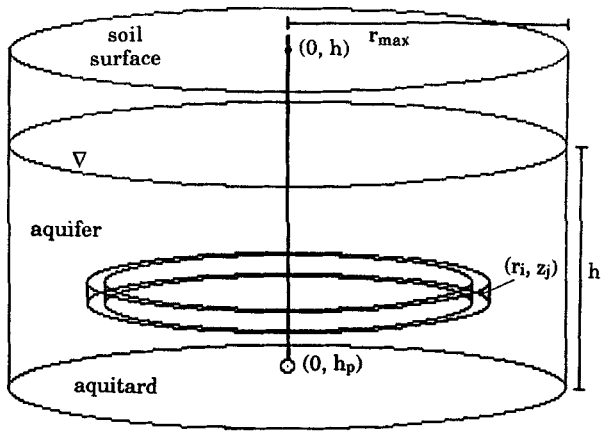

FIG. 1 Geometry and notation of a single vertical sparging well screened near the bottom.

The calculation of fluid flow in such multiphasic systems is a formidable task which we shall avoid by postulating the z-components of the air and water fluxes and then calculating the r-components from conservation requirements. This portion of our analysis differs somewhat from that for the horizontal pipe model, so will be presented in detail. The equations describing advective transport in the mobile water are slightly more complex than in the previous model, and will be treated fully. The equations describing solution of NAPL droplets and diffusion through the immobile water in the clay lenses to the mobile water are virtually identical to those derived in connection with the previous model and will be presented without proof.

The Gas Flow Field

Our development of the gas flow field here follows along the same lines as those used in the horizontal pipe model, except for the fact that here cylindrical coordinates are employed whereas there Cartesian coordinates were used. We postulate the following expression for the z-component of the molar gas flux:

$$\begin{aligned} q_z &= A(z)[a_0^2(z/h) - r^2], \qquad r < a_0(z/h)^{1/2} = r' \\ &= 0, \quad r > r' \end{aligned} \tag{1}$$

where a_0 is the maximum radial distance from the well at the top of the aquifer (where $z = h$) at which gas appears. The function $A(z)$ is calculated

from the requirement that the total molar gas flow, Q, must be given by

$$Q = \int_0^{2\pi} \int_0^{r'} A(z)[r'^2 - r^2] r \, dr \, d\theta \tag{2}$$

which yields

$$A(z) = \frac{2Qh^2}{\pi a_0^4 z^2} \tag{3}$$

So

$$q_z = \frac{2Qh^2}{\pi a_0^4 z^2} [a_0^2(z/h) - r^2] \tag{4}$$

It is next necessary to determine the radial component of the molar gas flux, q_r. This is done by noting that $\mathbf{q}$ is conservative, so

$$\nabla \cdot \mathbf{q} = 0 \tag{5}$$

For our geometry this gives

$$\frac{1}{r} \frac{\partial}{\partial_r} (rq_r) + \frac{\partial q_z}{\partial z} = 0 \tag{6}$$

From Eqs. (4) and (6) we obtain

$$\frac{\partial}{\partial r} (rq_r) = -\frac{2Qh^2}{\pi a_0^4} \left[\frac{a_0^2 r}{hz^2} + \frac{2r^3}{z^3} \right] \tag{7}$$

Integration of this equation from 0 to r and division by r then yields

$$q_r = \frac{Qh^2 r}{\pi a_0^4 z^3} [a_0^2(z/h) - r^2] \tag{8}$$

What is needed is the volumetric gas flux rather than the molar gas flux. We assume that the pressure at (r, z) is adequately approximated by the sum of the ambient pressure P_a (1 atmosphere) and the hydrostatic pressure, so

$$P(z) = P_a + \eta(h - z) \qquad (\eta = 0.09675 \text{ atm/m}) \tag{9}$$

Then the components of the volumetric gas flux are given by

$$U_r = q_r RT/P(z) \tag{10}$$

and

$$U_z = q_z RT/P(z) \tag{11}$$

The Water Circulation

We postulate for the z-component of the water superficial velocity $\mathbf{v}$ the expression

$$v_z = Bz(h - z)(b - r) \exp(-cr) \tag{12}$$

where B, b, and c are constants to be determined or assigned. This expression makes v_z positive near the well, negative at distances greater than b from the well, zero at $z = 0$ and at $z = h$, and 0 in the limit of large r. These properties are qualitatively what one would expect for the water circulation around a sparging well.

It is necessary that the total flux of water through any horizontal plane be equal to zero, since there are no sources or sinks of water in the vicinity. Therefore we must have

$$\int_0^{2\pi} \int_0^{\infty} v_z r \, dr \, d\theta = 0 \tag{13}$$

Substitution of Eq. (12) into Eq. (13) yields the requirement that

$$\int_0^{\infty} (b - r) r \exp(-cr) \, dr = 0 \tag{14}$$

from which we find that c must be given by

$$c = 2/b \tag{15}$$

and so

$$v_z = Bz(h - z)(b - r) \exp(-2r/b) \tag{16}$$

The r-component of the water circulation field is obtained by the method employed above to get q_r. Since the field is conservative,

$$\nabla \cdot \mathbf{v} = 0 \tag{17}$$

This gives

$$r^{-1} \frac{\partial}{\partial r} (r v_r) = -\frac{\partial v_z}{\partial z} = -B(h - 2z)(b - r) \exp(-2r/b) \tag{18}$$

Multiplication by r, integration from 0 to r, and division by r then yields

$$v_r = -(Bb/2)(h - 2z) r \exp(-2r/b) \tag{19}$$

This completes the calculation of the superficial velocity field for the water circulation. A representative set of streamlines for the water circula-

tion is shown in Fig. 2; the time periods for points on these streamlines to make a complete circuit are indicated in the legend.

Advective Transport of VOC

In sparging, advective transport takes place in both the gaseous and the mobile aqueous phases. The ring-shaped volume elements which will be used are shown in Fig. 1. We assume that the gas phase and the mobile aqueous phases are in local equilibrium, which gives

$$C_{ij}^{g} = K_{\mathrm{H}} C_{ij}^{m} \tag{20}$$

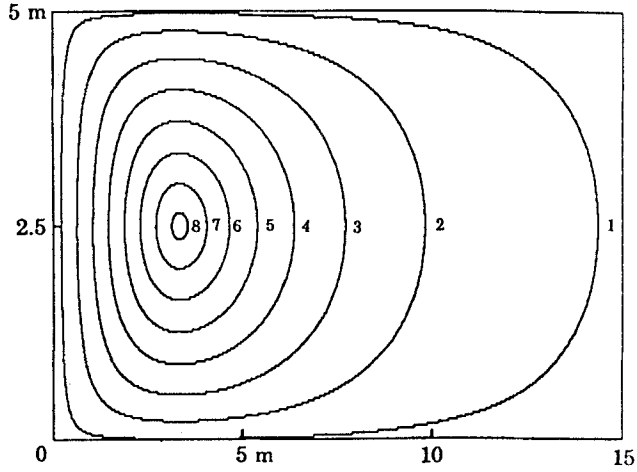

FIG. 2 Streamlines calculated for the water circulation flow field. The times required to make a circuit for each streamline are as follows:

Trajectory number	Transit time (days)
1	185.32
2	20.48
3	8.42
4	5.16
5	3.84
6	3.22
7	2.92
8	2.80

The distance b from the axis of the system to the stagnation point is 3.33 m. The water circulation scale factor $B = 0.4/86{,}400\ \mathrm{m^{-2} \cdot s^{-1}}$, and $\omega^{m} = 0.2$.

Here C_{ij}^g = gas phase VOC concentration in the ijth volume element, kg/m^3
C_{ij}^m = VOC concentration in the mobile aqueous phase in the ijth volume element, kg/m^3
K_H = Henry's constant for the VOC, dimensionless

The volume of the ijth volume element is given by

$$\Delta V_{ij} = (2i - 1)\pi(\Delta r)^2\Delta z \tag{21}$$

The Top, Bottom, Inner, and Outer surfaces of this volume element are given by

$$S_{ij}^T = S_{ij}^B = (2i - 1)\pi(\Delta r)^2 \tag{22}$$

$$S_{ij}^I = 2\pi(i - 1)\Delta r\Delta z \tag{23}$$

$$S_{ij}^O = 2\pi i\Delta r\Delta z \tag{24}$$

Let

ω^m = mobile water porosity

ω^i = immobile water porosity

A mass balance on VOC transported in the gas phase then gives

$$\begin{aligned}\omega^m\Delta V_{ij}\left[\frac{dC_{ij}^m}{dt}\right]_{\text{gas}} &= K_H S_{ij}^I U_{ij}^I [S(U^I)C_{i-1,j}^m + S(-U^I)C_{ij}^m] \\ &+ K_H S_{ij}^O U_{ij}^O [-S(-U^O)C_{i+1,j}^m - S(U^O)C_{ij}^m] \\ &+ K_H S_{ij}^B U_{ij}^B \left[S(U^B)C_{i,j-1}^m \frac{P[(j-1)\Delta z]}{P[(j-3/2)\Delta z]}\right. \\ &\left. + S(-U^B)C_{ij}^m \frac{P[(j-1)\Delta z]}{P[(j-1/2)\Delta z]}\right] \\ &+ K_H S_{ij}^T U_{ij}^T \left[-S(-U^T)C_{i,j+1}^m \frac{P[j\Delta z]}{P[(j+1/2)\Delta z}\right. \\ &\left. - S(U^T)C_{ij}^m \frac{P[j\Delta z]}{P[(j-1/2)\Delta z]}\right]\end{aligned} \tag{25}$$

where

$S(u) = 0, \quad u < 0$
$= 1, \quad u \geq 0,$ and

$$U_{ij}^I = U_r[(i - 1)\Delta r, (j - 1/2)\Delta z] \tag{26}$$

$$U_{ij}^O = U_r[i\Delta r, (j - 1/2)\Delta z] \tag{27}$$

$$U_{ij}^{B} = U_z[(i - 1/2)\Delta r, (j - 1)\Delta z] \tag{28}$$

$$U_{ij}^{T} = U_z[(i - 1/2)\Delta r, j\Delta z] \tag{29}$$

give the gas fluxes at the four surfaces of the volume element. Note that here we have included pressure correction terms to take into account the expansion of the gas as it rises from the bottom surface of the volume element to its center or from the center to the top.

Similarly, a mass balance on VOC transported in the mobile aqueous phase gives

$$\begin{aligned}\omega^m \Delta V_{ij} \left[\frac{dC_{ij}^m}{dt}\right]_{\text{water}} &= S_{ij}^{I} v_{ij}^{I} [S(v^{I})C_{i-1,j}^m + S(-v^{I})C_{ij}^m] \\ &+ S_{ij}^{O} v_{ij}^{O} [-S(-v^{O})C_{i+1,j}^m - S(v^{O})C_{ij}^m] \\ &+ S_{ij}^{B} v_{ij}^{B} [S(v^{B})C_{i,j-1}^m + S(-v^{B})C_{ij}^m] \\ &+ S_{ij}^{T} v_{ij}^{T} [-S(-v^{T})C_{i,j+1}^m - S(v^{T})C_{ij}^m]\end{aligned} \tag{30}$$

where

$$v_{ij}^{I} = v_r[(i - 1)\Delta r, (j - 1/2)\Delta z] \tag{31}$$

$$v_{ij}^{O} = v_r[i\Delta r, (j - 1/2)\Delta z] \tag{32}$$

$$v_{ij}^{B} = v_z[(i - 1/2)\Delta r, (j - 1)\Delta z] \tag{33}$$

$$v_{ij}^{T} = v_z[(i - 1/2)\Delta r, j\Delta z] \tag{34}$$

Solution of NAPL Droplets

The solution of NAPL droplets distributed within the low-permeability lenses is handled in exactly the same fashion as in our earlier work (3). Transcription to the notation used with the cylindrical geometry employed here gives

$$\frac{dm_{ijk}}{dt} = -\frac{3\Delta V_{ij} C_0^N D(C_{\text{sat}} - C_{ijk}^i)(m_{ijk}/m_{ij}^0)^{1/3}}{n_u a_0'^2 \rho_{\text{voc}}[1 - (a_0'/d)(m_{ijk}/m_{ij}^0)^{1/3}]} \tag{35}$$

Here n_u = number of slabs into which the low-permeability clay lenses are partitioned for mathematical analysis

m_{ijk} = mass of NAPL in the kth slab of immobile water in the ijth volume element, kg

$m_{ij}^0 = C_0^N \Delta V_{ij}/n_u$ = initial mass of NAPL in the kth slab, kg

C_0^N = initial NAPL concentration in the contaminated region, kg/m^3

a_0' = initial radius of NAPL droplets, m

$d - a$ = boundary layer thickness around NAPL droplet, m; d estimated from Eq. (36).

D = diffusion constant of VOC in the immobile aqueous phase, m^2/s. This includes the molecular diffusivity of the VOC in water, the tortuosity, etc.
C_{sat} = aqueous solubility of VOC, kg/m^3
ρ_{voc} = density of VOC, kg/m^3
C^i_{ijk} = VOC concentration in the immobile aqueous phase in the kth slab of the ijth volume element, kg/m^3

In Reference 3 it was shown that a reasonable value for the outer radius of the boundary layer thickness around a NAPL droplet is given by

$$d = a'_0 \left[\frac{\pi\omega\rho_{voc}}{6C_0^N}\right]^{1/3} \tag{36}$$

Diffusion of VOC through the Immobile Water in the Clay Lenses

This, also, is handled as in Reference 3. With minor notation changes to accommodate cylindrical geometry, the equations become

$$\frac{dC^i_{ijk}}{dt} = \frac{D}{(\Delta u)^2 v_{clay}}(C^i_{ij,k+1} - 2C^i_{ijk} + C^i_{ij,k-1}) - \frac{n_u}{\omega^i \Delta V_{ij}}\frac{dm_{ijk}}{dt}, \tag{37}$$

$$k = 2, 3, \ldots, n_u - 1$$

$$\frac{dC^i_{ijnu}}{dt} = \frac{D}{(\Delta u)^2 v_{clay}}(-C^i_{ijnu} + C^i_{ij,nu-1}) - \frac{n_u}{\omega^i \Delta V_{ij}}\frac{dm_{ijnu}}{dt} \tag{38}$$

and

$$\frac{dC^i_{ij1}}{dt} = \frac{D}{(\Delta u)^2 v_{clay}}[C^i_{ij2} - C^i_{ij1} + 2(C^m_{ij} - C^i_{ij1})] - \frac{n_u}{\omega^i \Delta V_{ij}}\frac{dm_{ij1}}{dt} \tag{39}$$

Here $2l$ = thickness of the clay lenses, m
Δu = thickness of a slab of immobile water in the clay lenses, m ($\Delta u = l/n_u$)
v_{clay} = porosity of clay in the low-permeability lenses

Completion of the Mobile Aqueous Phase Material Balance

The term modeling diffusion of VOC from the first immobile aqueous layer in the lenses ($k = 1$) into the mobile aqueous phase is

$$\omega^m \Delta V_{ij}\left[\frac{dC^m_{ij}}{dt}\right]_{diff} = \frac{\omega^i \Delta V_{ij} D}{l v_{clay}(\Delta u/2)}(C^i_{ij1} - C^m_{ij}) \tag{40}$$

The overall material balance for VOC in the mobile aqueous phase is then given by

$$\frac{dC_{ij}^m}{dt} = \left[\frac{dC_{ij}^m}{dt}\right]_{\text{gas}} + \left[\frac{dC_{ij}^m}{dt}\right]_{\text{water}} + \left[\frac{dC_{ij}^m}{dt}\right]_{\text{diff}} \tag{41}$$

The Model

The model then consists of the following differential equations. The change of mass of NAPL in the kth slab of the ijth volume element is governed by Eq. (35). The VOC concentration in the immobile water in the kth slab of the ijth volume element is calculated from Eqs. (37), (38), or (39). Finally, the VOC concentration in the mobile water in the ijth volume element is calculated by means of Eq. (41), which is in turn composed of Eqs. (25), (30), and (40).

Initialization consists of specifying the model parameters, and the dimensions of the contaminated zone and the initial VOC concentration in the contaminated zone. The differential equations were then integrated forward in time by the simple Euler formula, since RAM restrictions precluded using a more sophisticated method.

The total mass of residual VOC in the domain of interest at any time t is given by

$$M_{\text{tot}} = \sum_{i=1}^{n_r} \sum_{j=1}^{n_z} \left[\Delta V_{ij} \omega^m C_{ij}^m + \sum_{k=1}^{n_u} (m_{ijk} + (\omega^i \Delta V_{ij}/n_u) C_{ijk}^i) \right]$$

In the runs to be presented in the next section, we shall plot a reduced total mass, $M' = M_{\text{tot}}(t)/M_{\text{tot}}(0)$.

We shall also be interested in the rebound of the VOC concentration in the mobile aqueous phase after the sparging well has been shut off. The modeling equations for the system after sparging has been stopped are exactly the same as those given above, except that the gaseous and aqueous advection terms are dropped. One can then plot reduced concentrations at various points within the domain, defined by $C'_w = C_{ij}^m/C_{\text{sat}}$, where w is an index indicating the values of i and j being used.

RESULTS

The model was implemented in TurboBASIC and run on a microcomputer using a 80486 microprocessor and having a clock speed of 50 MHz. A typical run required about 9 minutes of computer time after the run parameters were input.

Default parameters for the runs are given in Table 1. Variations from this set of values are indicated in the text and figure legends as they occur.

Before exploring other aspects of the model it is necessary to determine how large the radius of the domain of interest must be to avoid spurious losses of VOC by the washing of VOC out of the domain of interest by the water circulation. Physically, of course, this VOC is not removed from the aquifer, but is only spread out; the domain of interest must be chosen large enough so that this washout effect is negligible. Runs in which the air flow rate is set equal to zero while water circulation takes place allow one to investigate this point. In Fig. 3 we see that, for runs made with the default parameters, a domain radius of 10 m permits a little washout to occur in the course of a 30-day run, but that a domain radius of 15 m shows no evidence whatever of washout. Therefore a domain radius of 15 m was used throughout.

TABLE 1
Default Parameters for Sparging Runs, Single Vertical Well

Thickness of aquifer	5 m
Height of screened section of well above aquitard	0.5 m
Molar air flow rate to well	0.4 mol/s
(Volumetric air flow rate	20.7 SCFM)
Radius of influence of air at top of aquifer, a_0	5 m
Distance of center of water circulation from well axis, b	3.33 m
Radius of domain of interest, r_{max}	15 m
Scale factor for water circulation, B	0.4/86,400 (1/m^2·s)
Temperature	25°C
Mobile water-filled porosity, ω^m	0.2
Immobile water-filled porosity, ω^i	0.2
Soil density	1.7 g/cm^3
Identity of VOC	Trichloroethylene, TCE
Density of VOC, ρ_{voc}	1.46 g/cm^3
Aqueous solubility of VOC	1100 mg/L
Henry's constant of VOC (dimensionless)	0.2821
Diffusivity of VOC in immobile water, D	2×10^{-10} m^2/s
n_r	15
n_z	5
Thickness of clay lenses, $2l$	1 cm
Porosity of clay lenses, ν_{clay}	0.4
Number of slabs into which lenses are partitioned for mathematical analysis	5
Initial total VOC concentration	2000 mg/kg
Initial NAPL droplet diameter, $2a_0'$	0.1 cm
Radial distance to which contamination extends	4 m
Depth in aquifer to which contamination extends	4 m
Δt	225 seconds

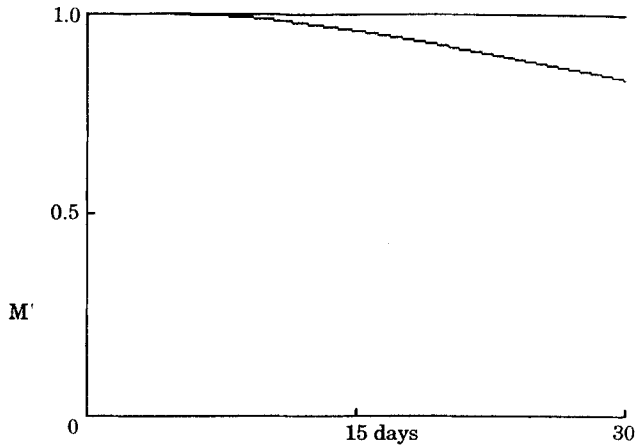

FIG. 3 Plots of M' versus time; the "wash-out" effect. The air flow rate $Q = 0$; $r_{max} =$ 15, 10 m from the top down. Other parameters as in Table 1.

For a horizontal slotted pipe sparging well configuration, we found earlier (3) that the half-width of the domain of interest had to be at least 25 m to avoid significant washout. The difference between the two geometries appears to be associated with the exponential attenuation factors of the water circulation velocity components. For the horizontal slotted pipe system the derived exponential attenuation factor is $\exp(-x/b)$, where b is the distance of the center of circulation from the axis of the system. For the vertical well configuration considered here, our derivation yielded an exponential attenuation factor of $\exp(-2r/b)$, which attenuates with distance from the well substantially more rapidly.

Figure 4 shows a comparison of sparging runs made with a single vertical well (V) and a single horizontal well (H) with identical gas flow rates, values of a_0 (maximum distance to which the gas flux extends laterally from the well), b, etc. To our surprise, the vertical well performed substantially more efficiently than did the horizontal slotted pipe, even when one takes into account the smaller volume of the domain of interest of the vertical well (201 m^3 compared to 320 m^3 for the horizontal well). Examination of the mobile aqueous VOC concentration values in the domains of interest provided the explanation for this result. The influence of the water circulation field for the horizontal well extends out laterally much farther than does that of the water circulation field for the vertical well, as a result of the difference in exponential attenuation factors. This results in substantial quantities of VOC being carried far out of the aeration zone

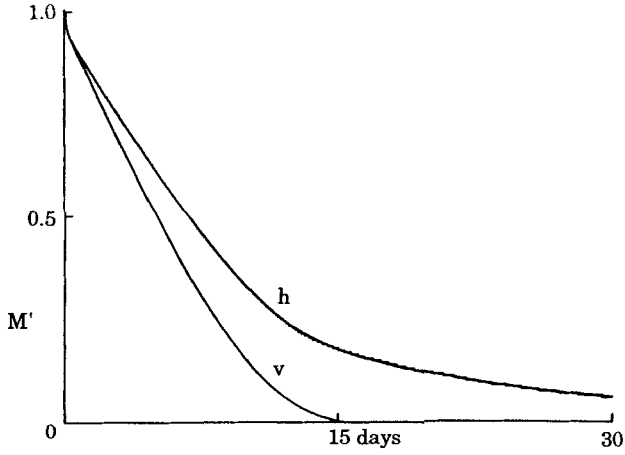

FIG. 4 Plots of M' versus time; comparison of the performances of a single vertical well V (all parameters as in Table 1) and a single horizontal slotted pipe well (length of pipe = 10 m, air flow rate = 0.4 mol/s, water circulation scale factor B' = 0.05/86,400 $m^{-2} \cdot s^{-1}$, other parameters as in Table 1).

of the horizontal well. Before this VOC can be removed, it must be carried by water advection back into the aeration zone, which is a slow process. This is responsible for the extensive tailing shown by the horizontal slotted pipe well results. In soil vapor extraction the relative efficiencies of the two well configurations are just the opposite; in SVE there is no water circulation to spread the VOC out of the aeration zone.

The effect of linked air flow and water circulation rates is shown in Fig. 5. Here we have taken the water circulation rate parameter to be proportional to the air flow rate on the basis of some quite preliminary data on the aeration of a bench scale water-saturated sand bed. As one would intuitively expect, increased advection results in faster removal rates. However, this process is eventually limited by the rates of mass transfer of the solution and diffusion processes, so that the rate of cleanup is less than proportional to the air flow rate.

The effect of well depth is shown in Fig. 6. As the well depth is decreased, the expected decrease in removal rate and increase in the extent of tailing toward the end of the cleanup are clearly seen. As was also observed with horizontal sparging wells, it is unwise to attempt to economize by drilling shallow wells. Water circulation is not an efficient way to move VOC from the contaminated zone into the zone of aeration.

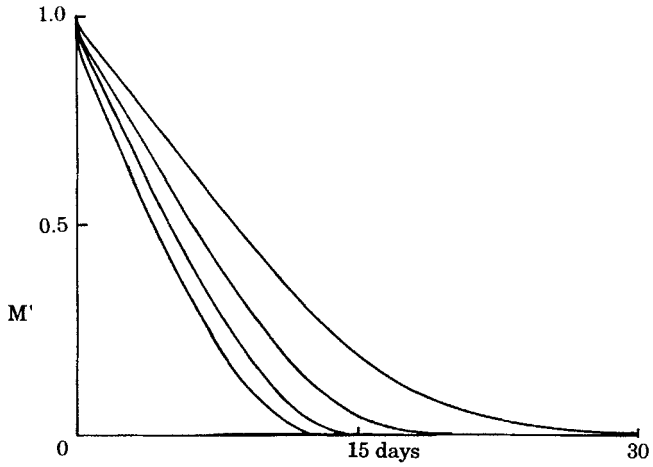

FIG. 5 Plots of M' versus time; effect of linked air flow rate and water circulation rate. (Q, 86,400B) = (0.1, 0.1), (0.2, 0.2), (0.4, 0.4), and (1.0 mol/s, 1.0 $m^{-2} \cdot s^{-1}$), from the top down.

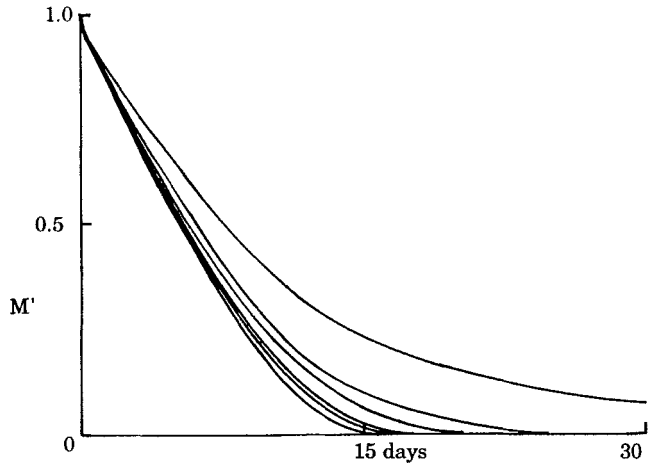

FIG. 6 Plots of M' versus time; effect of well depth. Height of well above the bottom of the aquifer = 3.0, 2.5, 2.0, 1.5, 1.0, and 0.5 m from the top down.

The effect of the maximum radius of the air flow field is shown in Fig. 7. A radius which is too small leaves some of the contaminated zone unaerated, so cleanup rate is reduced somewhat. A radius which is too large results in substantial amounts of air being wasted by moving through regions containing no contaminant, so again cleanup rate is reduced somewhat.

Figure 8 shows the very large effect which the thickness of the low-permeability lenses has on the rate of cleanup. Initially there is a period of a few hours during which removal rates are rapid, as dissolved VOC is removed from the mobile water by the sparging air. Shortly thereafter, however, diffusion from the clay lenses becomes the rate limiting factor, and cleanup rates decrease markedly, depending on the thickness of the clay lenses. The thicknesses of the lenses here range from 0.5 (rapid cleanup) to 3.0 cm (quite slow cleanup). One would be well advised to check the well logs for a site quite carefully for indications of the presence of such structures.

The effect of NAPL droplet radius a_0' on cleanup rate is also quite large, with cleanup rates decreasing with increasing droplet size (and correspondingly decreasing NAPL–water interfacial area). This is seen in Fig. 9. We note that the effects of increasing lens thickness and increasing droplet size are extremely similar, and that it would probably be impossible to distinguish between them on the basis of field pilot studies. On the

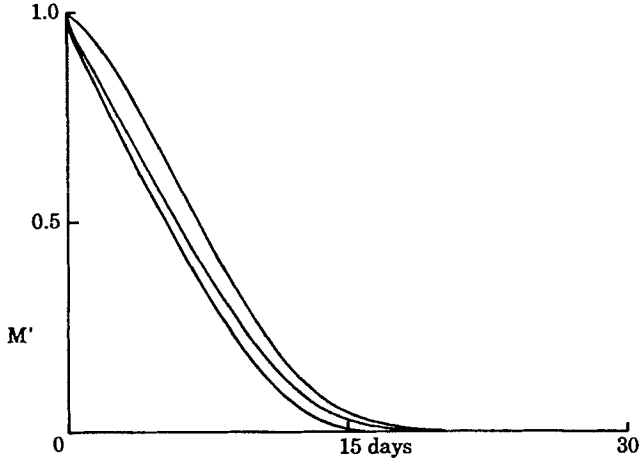

FIG. 7 Plots of M' versus time; effect of maximum radius of air distribution a_0. a_0 = 3, 8, and 5 m from the top down.

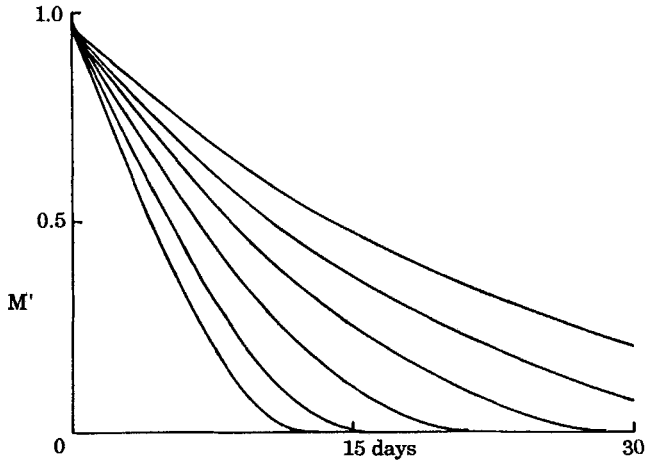

FIG. 8 Plots of M' versus time; effect of thickness of the low-permeability lenses, $2l$. $2l$ = 3.0, 2.5, 2.0, 1.5, 1.0, and 0.5 cm from the top down.

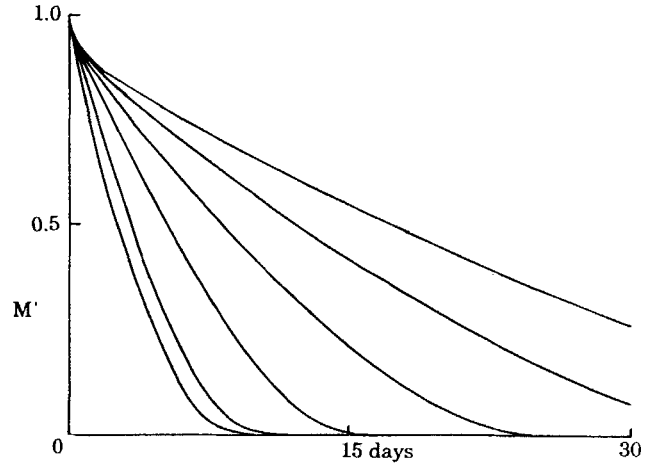

FIG. 9 Plots of M' versus time; effect of diameter of NAPL droplets, $2a_0'$. $2a_0'$ = 0.01, 0.02 (superimposed), 0.05, 0.10, 0.15, 0.20, and 0.25 cm from the bottom up.

other hand, since the effects are so similar, distinguishing between them is probably unnecessary for practical purposes.

In Figs. 10–13 we examine the phenomenon of rebound—the increase in VOC concentration in groundwater (or soil gas) after a remediation operation (sparging, pump-and-treat, SVE) has been terminated. We earlier explored the rebound phenomenon in connection with SVE (4).

Figure 10 shows plots of the reduced VOC mass and two reduced mobile water concentrations as functions of time. The concentration C_1' is the concentration of VOC in the mobile water at the top center of the zone of contamination; C_2' is the mobile water VOC concentration at the bottom outer edge of the zone of contamination. In Fig. 10 the run is carried out for 30 days, with cleanup being essentially complete after 15 days. As expected, C_1' is always less than C_2', since the top center of the zone of contamination receives a much larger air flux than does the bottom outer edge.

In Fig. 11 the sparging well is shut off after 12.5 days, shortly before remediation is complete. The rebound of C_1' is negligible, indicating that this portion of the zone of contamination is essentially cleaned up. Rebound of C_2', however, is appreciable, although not large. Evidently the aquifer near the lower outer edge of the zone of contamination no longer

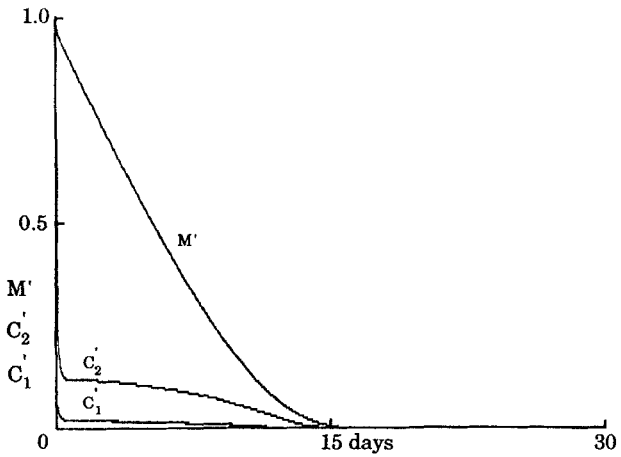

FIG. 10 Plots of M', C_1', and C_2' versus time. C_1' is the reduced concentration of VOC in the mobile water at the top center of the zone of contamination. C_2' is the reduced concentration of VOC in the mobile water at the bottom outer edge of the zone of contamination. All parameters as in Table 1.

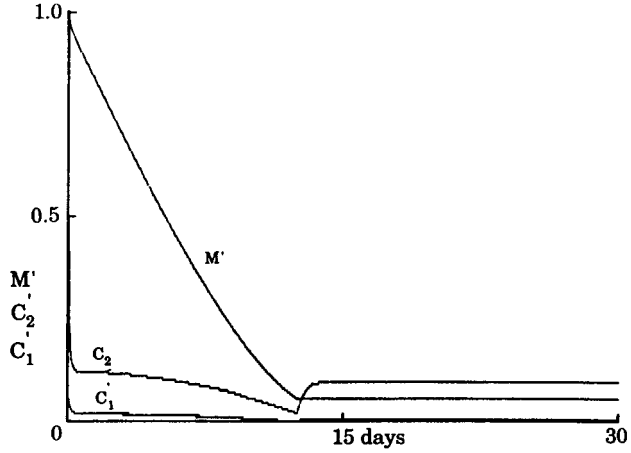

FIG. 11 Plots of M', C_1', and C_2' versus time. The sparging well was shut down after 12.5 days of operation.

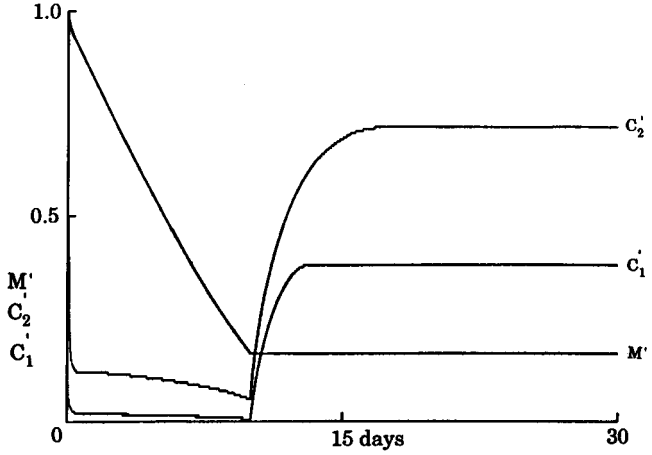

FIG. 12 Plots of M', C_1', and C_2' versus time. The sparging well was shut down after 10 days of operation.

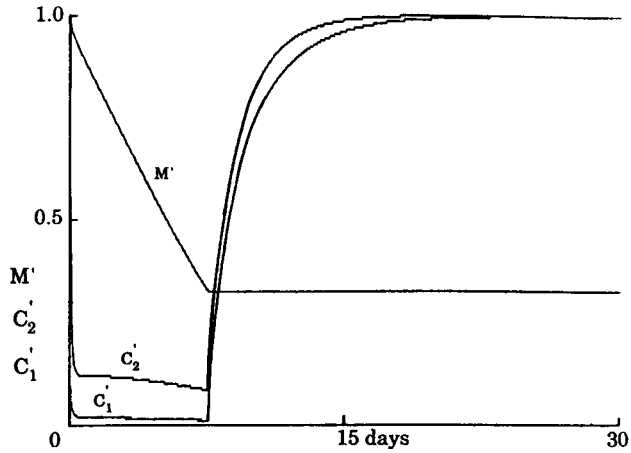

FIG. 13 Plots of M', C_1', and C_2' versus time. The sparging well was shut down after 7.5 days of operation.

contains NAPL (or rebound would be much larger), but there is still some dissolved VOC diffusing from the immobile water in the clay lenses.

Rebound is quite a bit larger in Fig. 12, in which the sparging well is shut down after 10 days of operation. Both C_1' and C_2' show substantial rebound, with C_1' recovering to a value less than that to which C_2' recovers. As noted above, this is expected because of the difference in air flux through the two portions of the contaminated zone.

Rebound in Fig. 13, for which run the sparging well was turned off after 7.5 days of operation, is the maximum possible for both C_1' and C_2', indicating that NAPL is still present in both portions of the contaminated zone.

CONCLUSIONS

The following conclusions can be drawn from the results obtained with this sparging model.

- Somewhat surprisingly, vertical sparging wells appear to be rather more efficient than horizontal slotted pipe sparging wells, in that one does not have nearly as much tailing of the cleanup with the vertical wells as one has with the horizontal wells. This is apparently due to the increased range of the water circulation field for the horizontal wells as compared to that for the vertical wells.

- Sparging wells should be drilled all the way through the zone of contamination to achieve maximum cleanup rates.
- Increasing air flow rates result in increased cleanup rates, but diffusion and solution mass transfer rates eventually become rate limiting. At that point, further increases in air flow rate are futile.
- NAPL droplet size and low-permeability lens thickness are extremely important in limiting diffusion and solution mass transfer rates.
- Diffusion and solution kinetics result in a rebound in the mobile water VOC concentrations after a sparging well is shut down. The magnitude of this rebound depends on the location at which the water sample is taken and the extent to which the overall cleanup has progressed. Rebound can be expected to be largest in those contaminated regions which receive the lowest flux of air.

ACKNOWLEDGMENTS

D.J.W. is greatly indebted to the University of Málaga for its hospitality and use of its facilities, to Dr. J. J. Rodríguez-Jimenez for making his visit to Málaga possible and for discussions of the project, to Vanderbilt University for financial support during his leave, and to the Spanish Government (DGICYT) for a fellowship in support of this work.

REFERENCES

1. R. A. Brown, *Air Sparging: A Primer for Application and Design*, Groundwater Technology, Inc., 310 Horizon Center Dr., Trenton, New Jersey, 086911. Undated.
2. *Symposium on Soil Venting*, Houston, Texas, April 29–May 1, 1991, U.S. EPA Report EPA/600/R-92/174, 1992.
3. D. J. Wilson, J. M. Rodríguez-Maroto, and C. Gómez-Lahoz, "Groundwater Cleanup by In-Situ Sparging. VI. A Solution/Distributed Diffusion Model for Nonaqueous Phase Liquid Removal," *Sep. Sci. Technol.*, *29*, 1401 (1994).
4. C. Gómez-Lahoz, J. M. Rodríguez-Maroto, D. J. Wilson, and K. Tamamushi, "Soil Cleanup by In-Situ Aeration. XV. Effects of Variable Air Flow Rates in Diffusion-Limited Operation," Ibid., *29*, 943 (1994).

Received by editor December 20, 1993